POLITECNICO
MILANO 1863

SCUOLA DI INGEGNERIA INDUSTRIALE
E DELL'INFORMAZIONE

Executive Summary of the Thesis

Analysis and Thermal Design of a Two-Level SiC Three-Phase Inverter

Laurea Magistrale in Electrical Engineering - Ingegneria Elettrica

Author: Giulio Santapà

Advisor: Prof. Francesco Castelli Dezza

Academic year: 2021-2022

1. Introduction

The student motorcycle team of Politecnico di Milano, called Polimi Motorcycle Factory, had been looking for the opportunity to have its own inverter for some time to provide their motorcycles with more power than they currently have. The old inverter was limited in current and sometimes had over temperature problems. The need to have more power available gave rise to this thesis project.
The thesis involves the study of the thermal behaviours and dimensioning of the power part of a three-phase inverter by analysing the MOSFETs thermal management, the CAD modelling and characterisation of a heatsink,
The heat sink has the task of keeping the MOSFETs below the maximum junction temperature. Using F.E.M software such as Ansys Icepack [1] and a simulation tool like Matlab [2], it was possible to study various aspects of the system. Such as the creation of a thermal model developed on Ansys and the creation of an electro-thermal model developed on Matlab thanks to the results found on the F.E.M. software. The two-level three-phase inverter uses silicon carbide (SiC) MOSFETs.
The need to use SiC MOSFETs derives from their properties and peculiarities, which, unlike their predecessors developed with Si technology, allow better heat management and guarantee improved performance.
The system that has been designed involves the use of 60 SiC modules, arranged with 10 MOSFETs in parallel for each high-side or low-side in the three phases. In this way it is possible to handle a high current and a low voltage. The low voltage is imposed by the motor which is a three-phase permanent magnet synchronous machine and it has a phase voltage of 120 V, with power up to 50 kW: therefore, the current handled is very high. The organizers provide the same engine to each team, so that the starting point is the same for everyone.
The data of the motor are reported in figure 1 and 2.

Nominal Operation			
Torque	T_{nom}	50	Nm
Power	P_{nom}	22	kW
Speed	n_{nom}	5500	rpm
Phase rms-current	I_{nom}	250	A
Battery voltage (DC)	U_{nom}	100	V
Electric frequency	$f_{el,nom}$	TBA	Hz
Power factor	cos(ϕ)	TBA	

Figure 1: Nominal values of the motor

Maximal Values			
Torque	T_{max}	120	Nm (2min)
Power	P_{max}	48	kW (2min)
Speed	n_{max}	7500	rpm
Phase rms-current	I_{max}	600	A
Battery voltage (DC)	U_{max}	140	V
Electric frequency	$f_{el,max}$	TBA	Hz

Figure 2: Maximum values of the motor

2. F.E.M. Studies

The study carried out on Ansys Icepack addressed the dimensioning of the heat exchanger. Starting with the creation of the thermal network of each MOSFET, the dimensioning of the exchanger was done.
There are constraints on the base, because the available space is already defined, these are:

- Base length equals to 300 mm
- Base width equals to 200 mm

Considering that the overall dimensions of the aluminum structure were already defined, the parameters concerning the fins and the vertical overall dimensions were obtained.
The heat sink parameters were derived once the junction temperatures of each individual MOSFET were below the datasheet limits of 175°C.
The results lead to the following geometry:

Size of the heat sink

Parameter	Value	Unit
Number of fins	28	/
Height of the fins	48	mm
Fin thickness	2	mm
Base 1 thickness	7	mm
Base 2 thickness	5	mm

Table 1: Size of the heatsink

Figure 3 shows the heat sink CAD model.

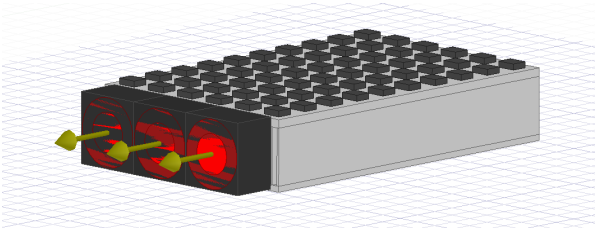

Figure 3: CAD model of the Heatsink

Before getting to the final model, many tests were done with the object to reduce the temperature; the model represented shows a double base, the second one is placed below the fins. Thanks to this base, it was possible to increase the power dissipated by each module by a few watts, reaching a dissipation of 70 W per modules.

2.1. Steady State and Transient Simulations

To define the goodness of the heatsink, steady state tests were done, where a maximum power dissipation was set. The test is conducted up to a steady state. The solver compares values called residuals, when these values reach a certain set threshold, the simulation stops. It reports the different values of the residuals of the equations it is calculating. It is possible to derive several quantities in the simulations, the ones that were most taken into account were the air velocity and the temperature on the surface of the structure.
In figure 4 is possible to see the outcome of a steady state virtual test.

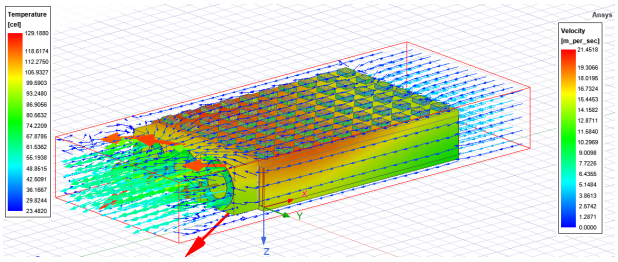

Figure 4: Final version of the Heatsink with height of the fins of 48 mm and back plate of 5 mm. A dissipation of 60 W per MOSFET was considered.

To determine the time interval elapsed before reaching the steady state temperature as well as the evloution of the observed physical quantities, transient tests were performed. In this way it is possible to estimate the time constant of the heat exchanger. In figure 5 there is the transient analysis result, it shows 10 curves of the temperature of a single column of MOSFETs. More precisely the high side of phase A.

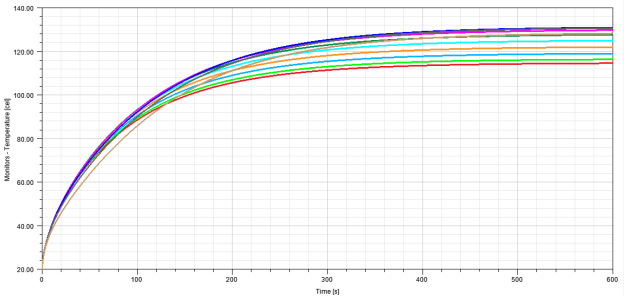

Figure 5: Transient test of the temperature of one MOSFETs columns

It can be seen that the time spent before reaching the steady state is 600 seconds, the time in which a constant power loss of 60 W per module is applied, the system dissipates an amount of 3600 W.
After the steady state and transient tests, the characterization of the heat exchanger was done.

2.2. Heat Sink Characterization

In order to characterize the heat exchanger thermal resistance, it was necessary to carry out several tests: a FEM model without fans was drawn, where precise boundary conditions are set. Tests were done at different airspeeds, which were set in correspondence of the air opening, and at constant power losses. In each test, the temperatures between every MOSFET and the heat exchanger was extracted.
Figure 6 reports the estimated thermal resistance of the heat sink as a function of the air speeds.

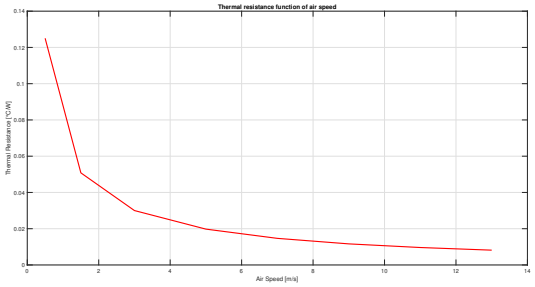

Figure 6: Characterization of the heat sink resistance, R_{ha} function of air speeds

It is possible to see how the thermal resistance of the heat sinks decreases as the speed of the incoming fluid increases. The reduction of R is visible up to values around 6-7 m/s: beyond that value the resistance does not drop so drastically. Nevertheless is difficult to bring air at that speed easily.

3. Electro-Thermal Model

The electro-thermal model was created in order to study different details. For example, it was not possible to directly change the power dissipated by each individual MOSFET.
This model was necessary because it has been seen that in thermal simulations, the temperatures recorded on the junctions are not constant on all modules. The MOSFETs close to the fans are affected by the heat removed by the previous modules. The result is that the temperature difference between MOSFETs on the same column, but at different heights, is over 20 degrees.
This model foresees the connection of 10 modules in parallel of a single side of the 6 that the three-phase inverter has.
The peculiarity of this model is to make the thermal and electrical model work at the same time and together, the ON state resistance and the junction temperature join the two circuits. Being $R_{DS_{ON}}$ dependent on the junction temperature it was possible to link the two models.
In the thermal network the losses injected are:

$$P_{CM} = R(T) \cdot I_{RMS}^2 \quad (1)$$

$$P_{SWM} = E(I_{RMS}) \cdot f_{sw} \quad (2)$$

$$P_{M_{tot}} = P_{CM} + P_{SWM} \quad (3)$$

$$P_D = R_d \cdot I_{RMS}^2 \quad (4)$$

The thermal network is reported in figure7, which models the thermal path of one single MOSFET. In the system there are 10 thermal networks:

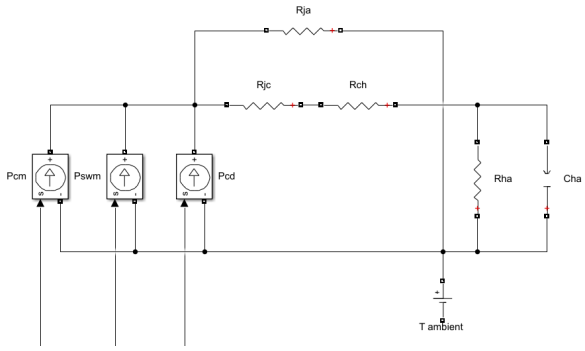

Figure 7: Thermal model of the Heat sink

The electrical network shown in the figure 8 represents a single column of the high side of the inverter for phase A. There are 10 resistors in parallel, that represent the 10 MOSFETs in parallel, while a single circuit model is created for the Diode as the variation of R_d with temperature is not very appreciable.
Figure 8 reports the electric model

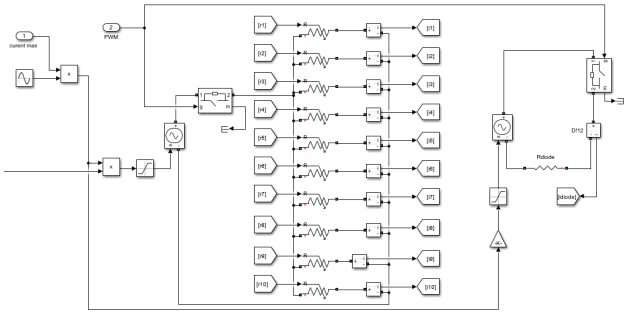

Figure 8: Electric model of the first MOSFETs column

With the electro-thermal network has been carried out two different tests: steady state used in order to study the effective junction temperatures and the dynamic test to study the temperature reached for a lap track.

3.1. Steady State Test

This test is done to see final temperatures with constant power consumption. The goal is to obtain uniform temperature distribution for all MOSFETs.
Hence, the current must suitably spread over the switches. If the current from the first module, which is at lower temperature, is higher than the current from the last then there may be a better temperature distribution in the system.
In figure 9 are reported the RMS values of the current of the first MOSFET and the last one in the column.

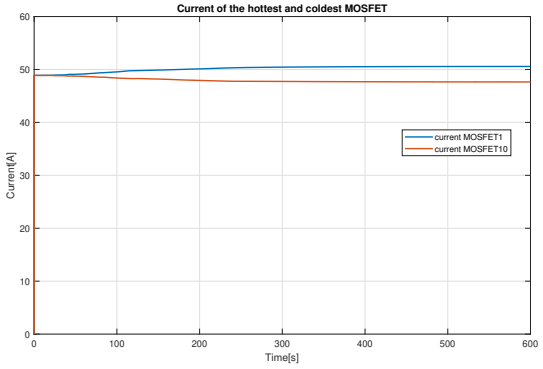

Figure 9: Current of the steady state test

In figure 10 is reported the power injected in the first MOSFET

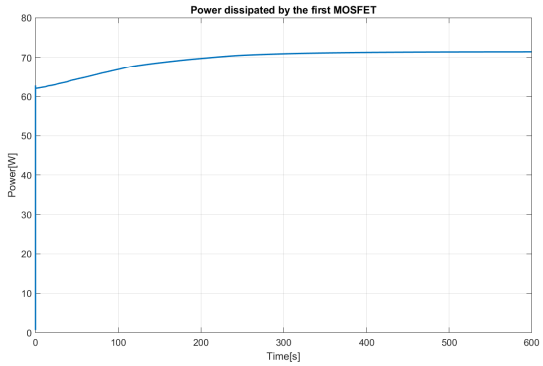

Figure 10: Current of the steady state test

The power injected reaches values higher than the one seen in Ansys Icepack, it is higher of almost 3 W.
In figure 11 are reported the ten curves of the junction temperatures of one column of MOSFETs of the high side of phase A.

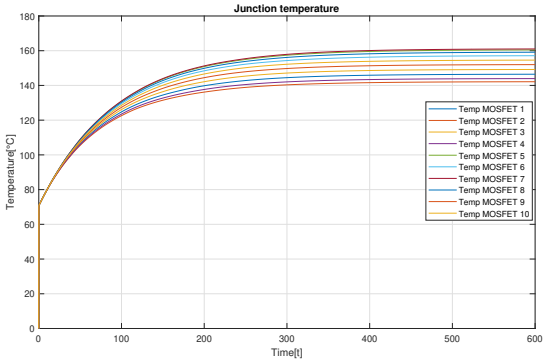

Figure 11: junction temperature of the first MOSFETs columun

Now the temperature of the 10 modules in the column actually reports better values than those obtained on Ansys Icepack. Indeed, the maximum value are lower than before, while the minimum has risen, here it is possible to say that the temperature has actually been redistributed. Even if the power is higher than the one set in Ansys Icepack the junction tempertures recorded are lower of 10 degrees. This temperature reduction is given by the current redistribution in the 10 MOSFETs.

3.2. Dynamic Test

This test is done in order to see the temperatures involved during a lap track. Using the same model as before, but imposing a vector of currents taken from the telemetry recorded dur-

ing a true run on the Imola track, in this way it has been done a dynamic test.
Here the test is done in order to see the effect of the damped peaks of the current.
The RMS of current absorbed by the MOSFETs are reported in the figure 12 below:

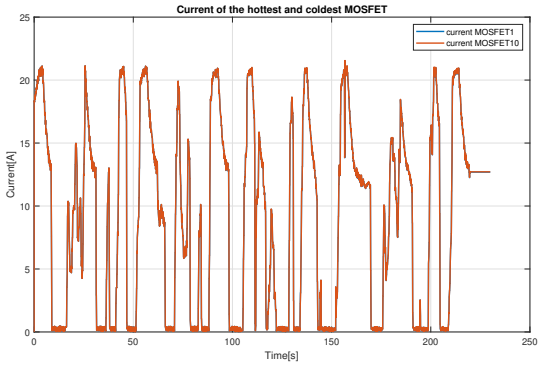

Figure 12: Current absorbed by the switches during the dynamic test

It is possible to see that the two values of current of the hottest and coldest MOSFET are almost equal.
In the figure 13 are reported the ten junction temperatures:

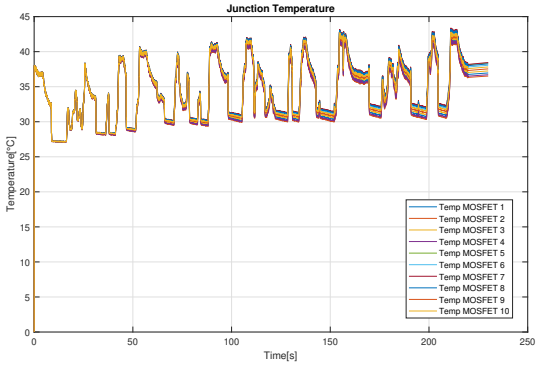

Figure 13: Junction temperature of the switches during the dynamic test

Here is possible to see that the values of temperature are almost similar. This is given by the low values of current.
This result shows how the junction heats up immediately when the current passes from zero to a very high value. When the current goes to zero, the junction temperature returns to the temperature of the heat exchanger, which in this case results in a very low value, which is at a temperature of about 30°C. The heat exchanger mass effect is appreciable when the applied current is zero. The heatsink temperature is reflected back to the junction temperature when the load is zero.

4. Electrical Test

The last test is the electrical test, it is used in order to see the electrical quantities involved in the inverter and their magnitude. So that is possible to define the power rating and the efficiency [3, 4].
The electric circuit is composed by 60 MOSFETs, 10 in parallel for each high side and 10 low side for each phases. The control uses Pulse width modulation technique, with a modulation ratio m_a equal to 1 and a m_f equal to 603.
The load used is a RL, with the value of the old motor used for the competition, that is:

- Rs=0.046 Ω
- Ls=96 μH

The scheme is reported in figure 14:

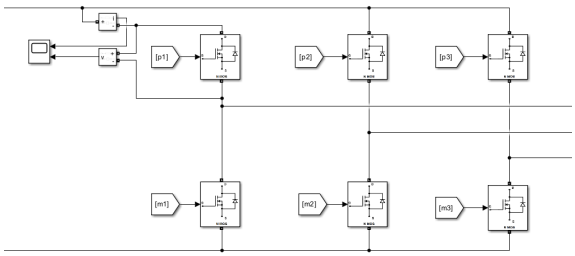

Figure 14: Two-level three-phase inverter

The three three-phase currents of the load with all the frequency components are reported in figure 15, and in figure 16 is reported the current ripple of the phase A.

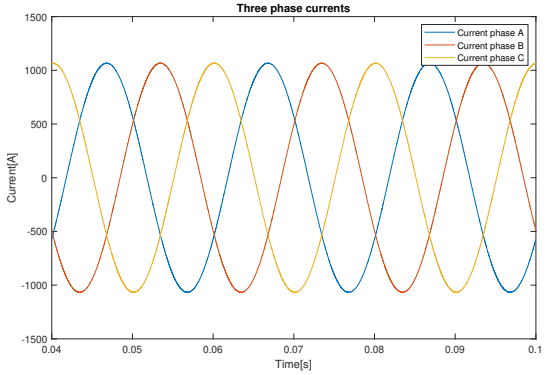

Figure 15: Three-phase currents

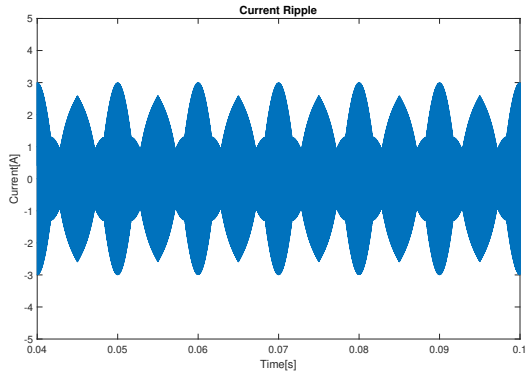

Figure 16: Current ripple of the phase A

It possible to see that the ripple is very low, only 3 A, with a current magnitude which is above one thousand A. The value of the ripple is low thanks to the high switching frequency of the MOSFETs. In this way is possible to reduce the ripple, but with high frequency the switching losses increase. In traction application, reducing the ripple results in a reduction of the torque ripple.
The phase voltage is reported in figure 17, the figure shows the phase voltage with all harmonics and the first harmonic voltage.

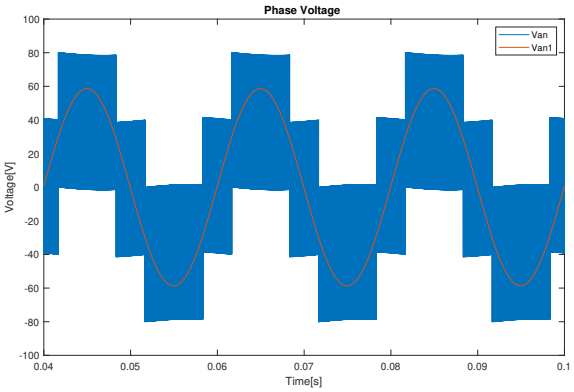

Figure 17: Phase voltage

It is possible to see the first harmonic of the phase voltage, and the voltage with all the hamonics content.
The total power handled by the system, is 81kW. The efficiency is calculated considering the losses among the switches, it is not the global efficiency because does not consider the drive circuit. The efficiency related to the power losses is equal to:

$$\begin{aligned}\eta &= \frac{P_{DC} - 60 \cdot (P_{CondMOS} + P_{SwMOS} + P_{CondD})}{P_{DC}} \\ &= \frac{81030W - 60 \cdot (36.6W + 6.0W + 18W)}{81030W} \\ &= 0.955 = 95.5\%\end{aligned}$$

Conclusions

Several virtual tests were carried out during this thesis work using two completely different software: Ansys Icepack and Matlab. The former made it possible to define the thermal specifications of the system, the latter made it possible to test a more dynamic and customisable model. The system thermally proved to be stable, in the full-scale test, it can guarantee a power dissipation per module of 70 W, ensuring that the inverter can control an electrical power of 80 kW. This power is sustained indefinitely by the aluminium heat sink.

References

[1] Ansys. Ansys icepack, 2023.

[2] Mathwork. Mathwork simulink, 2023.

[3] Robbins Mohan, Undeland. *Power Electronics*. John Wiley & Sons, 1995.

[4] Smith Sedra. *Microelectronic circuits*. Edises, 2019.

Acknowledgements

I would like to thank the professor Francesco Castelli Dezza and the Professor Nicola Toscani, I will also always be grateful to the professors that I had the chance to know in this fantastic route.